https://doi.org/10.5194/acp-2021-1006
Preprint. Discussion started: 5 January 2022

Atmospheric Chemistry and Physics Discussions

Volatility Parameterization of Ambient Organic Aerosols at a rural site of the Northern China Plain

Siman Ren[1], Lei Yao[1], Yuwei Wang[1], Gan Yang[1], Yiliang Liu[1], Yueyang Li[1], Yiqun Lu[1], Lihong Wang[1], Lin Wang[1,2,3,4]

[1]Shanghai Key Laboratory of Atmospheric Particle Pollution and Prevention (LAP[3]), Department of Environmental Science & Engineering, Jiangwan Campus, Fudan University, Shanghai 200438, China

[2] Collaborative Innovation Center of Climate Change, Nanjing, 210023, China

[3] Shanghai Institute of Pollution Control and Ecological Security, Shanghai 200092, China

[4] IRDR International Center of Excellence on Risk Interconnectivity and Governance on Weather/Climate Extremes Impact and Public Health, Fudan University, Shanghai 200438, China

Correspondence: Lin Wang (lin_wang@fudan.edu.cn)

ABSTRACT: The volatility of organic aerosols plays a key role in determining their gas-particle partitioning, which subsequently alters the physicochemical properties and atmospheric fates of aerosol particles. Nevertheless, an accurate estimation of the volatility of organic aerosols (OA) remains challenging. Because most standard particulate organic compounds are scarce, on the other hand, their vapor pressures are too low to estimate by most traditional methods. Here, we deployed an iodide-adduct Long Time-of-Flight Chemical Ionization Mass Spectrometer (LToF-CIMS) coupled with a Filter Inlet for Gases and AEROsols (FIGAERO) to probe the relationship between the molecular formulas of atmospheric organic aerosol's components and their volatilities. A number of T_{max} (*i.e.*, the temperature corresponding to the first signal peak of thermogram) were abstracted and validated from the desorption thermograms of mixed organic and inorganic calibrants which were atomized and then collected onto a Teflon filter. Besides, 30 filter samples of ambient air were collected in winter 2019 at Wangdu station in Beijing-Tianjin-Hebei region, and analyzed by FIGAERO-LToF-CIMS, leading to the identification of 1,448 compounds dominated by the CHO (containing carbon, hydrogen, and oxygen atoms) and CHON (containing carbon, hydrogen, oxygen, and nitrogen atoms) species. Among them, 181 organic formulas including 91 CHO and 90 CHON compounds were then selected since their thermograms can be characterized with clear T_{max} values in more than 20 out of 30 filter samples and subsequently divided into two groups according to their O/C ratios. The mean O/C of these two groups are 0.56 ± 0.35 (average ± one standard deviation) and 0.18 ± 0.08, respectively. We then obtained the correlation functions between volatility and elemental composition for the two group compounds. Compared with previous volatility parameterizations, our correlation functions provide a better estimation of the volatility of semi-volatility organic compounds (SVOCs) and low-volatility organic compounds (LVOCs) in the ambient organic aerosols. Furthermore, we suggest that there should be specialized volatility parameterizations for different O/C organic compounds.

1 Introduction

Aerosol particles can significantly impact human health, visibility and climate (Stocker et al., 2013). Organic aerosol (OA) comprises tens of thousands of organic substances and makes up a significant fraction of the total submicron particles in the troposphere (Nizkorodov et al., 2011). Whether an organic compound will exist in the gas phase or the particles under a specific temperature is determined by its volatility, which depends on its molar mass and functional groups (Capouet and Müller, 2006; Pankow and Asher, 2008). The volatility of a compound is usually expressed as saturation mass concentration (C^*) or saturation vapor pressure (*Psat*) (Donahue et al., 2011), and is regarded as one of the most critical physicochemical parameters for organic aerosols' components.

During the past years, three methods have been developed to characterize the volatility of aerosol particles. The first one estimates the volatility of an organic compound from its partitioning between the gas phase and the particle-associated phase.

https://doi.org/10.5194/acp-2021-1006
Preprint. Discussion started: 5 January 2022

Atmospheric Chemistry and Physics Discussions

Particulate fraction (F_p) for each organic compound can be calculated by measured gas phase and particle-associated concentrations or signals in the ambient atmosphere. Then F_p can be combined with the mass concentration of particulate OA, which was usually measured by an aerosol mass spectrometer (AMS) and temperature to estimate the C^* (Donahue et al., 2006; Pankow, 1994; Stark et al., 2017).

The second one estimates the volatility of an organic species from its molecular formula. The relationship between C^* and molecular formulas of seven categories of organic compounds including alkane, aldehyde, ketone, alcohol, acid, diol, and diacid was proposed based on a group contribution method SIMPOL (Pankow and Asher, 2008), which clarifies the relationship between n_C (the numbers of carbon) and n_O (the numbers of oxygen), and $\log C_0$ (C^* equals C_0 under the assumption of ideal thermodynamic mixing) (Donahue et al., 2011). Li et al.(2016) updated this function by including 31066 compounds from the National Cancer Institute (NCI) open database, which applies to not only CHO compounds (containing carbon, hydrogen, and oxygen atoms) but also the N- and S-containing compounds. On the other hand, Donahue et al. (2011) took only -OH, =O and -C(O)OH functionalities into account when describing an average effect of an added oxygen, which could result in a large uncertainty when estimating the volatility of highly oxygenated organic molecules (HOMs) that contain hydroperoxide (-OOH) functionalities. Thus, Stolzenburg et al. (Stolzenburg et al., 2018) and Mohr et al. (2019) updated the parameters for the volatility estimation of HOMs, based on 15 HOMs with known molecular structures and saturation concentrations (Tröstl et al., 2016). In addition, as the covalently bonded dimers are abundant in HOMs from ozonolysis of α-pinene, Stolzenburg et al. (2018) fit monomer and dimer HOMs separately, allowing the covalent binding to be an independent parameter. Since molecular formulas of organic aerosols can be obtained by state-of-the-art instruments such as high-resolution mass spectrometers, C^* of organic compounds in the aerosol particles can then be calculated based on the above-mentioned empirical function (Huang et al., 2019).

The third one estimates the volatility of an organic species from its desorption thermogram. When analyzing physicochemical properties of aerosol particles, one of the most popular techniques is to heat the particles and then detect the evaporated compounds utilizing mass spectrometry techniques, such as Thermodenuder-particle Beam Mass Spectrometer (Faulhaber et al., 2009), Thermal-Desorption Chemical Ionization Mass Spectrometer (TD-CIMS) (Smith et al., 2004), Micro-Orifice Volatilization Impactor Coupled to a Chemical Ionization Mass Spectrometer (MOVI-CIMS) (Yatavelli and Thornton, 2010), Chemical Analysis of Aerosols Online -Proton Transfer Reaction Mass Spectrometer (CHARON-PTR-MS) (Eichler et al., 2015), and the Filter Inlet for Gases and AEROsols (FIGAERO) coupled with Time-of-Flight Chemical Ionization Mass Spectrometer (ToF-CIMS) (Lopez-Hilfiker et al., 2014). Basically, the particulate organic compounds with different vapor pressures are characterized with distinct thermograms (i.e., the evolution of mass spectral signals in a range of desorption temperatures), and the temperature corresponding to the first peak signal (T_{max}) correlates with the vaporization enthalpy of a compound (Lopez-Hilfiker et al., 2014). It is thus applicable to estimate C^*, i.e., the volatility of the chemical constituents in the particles, from the measured T_{max}, after calibration with a set of standards with known vapor pressures (Bannan et al., 2019), which has been widely applied in many previous studies (Nah et al., 2019a; Stark et al., 2017; Wang et al., 2020a; Ye et al., 2019; Ylisirniö et al., 2019). Compared with the parameterization method from organic aerosols' molecular formulas, the thermogram method is able to give a volatility distribution that is closer to the real one, since the molecular formula method likely treats the thermal decomposition products as evaporated organic molecules after heating, and thus overestimated the overall volatility of a group of organics (Stark et al., 2017).

The FIGAERO-ToF-CIMS has been widely used in the field and laboratory studies in recent years. For example, Wang et al. (2020a) explored the volatility of aromatic hydrocarbon photo-oxidation products, Ylisirniö et al. (2019) compared the volatility of SOA (Secondary Organic Aerosol) components formed from oxidation of real tree emissions with that formed from oxidation of single VOC-systems, and Ye et al. (2019) studied the volatility of nucleated particles from α-Pinene oxidation between -50 ˚C and +25 ˚C using FIGAERO-ToF-CIMS. The success of this method depends on whether or not the desorption thermograms of the standards are accurately measured, which is yet under discussion. For example, previous studies typically used the syringe deposition method to prepare the mimic filter, which leads to wide variations in results. A new

https://doi.org/10.5194/acp-2021-1006
Preprint. Discussion started: 5 January 2022


Atmospheric Chemistry and Physics Discussions

method for volatility calibration, the atomization method, accurately captures the evaporation of chemical constituents from ambient aerosol particles (Ylisirniö et al., 2021). In addition, the influence of inorganic salts that are a major component in ambient aerosol particles on the thermograms of organics was not considered in these previous studies.

On the other hand, with rapid economic growth and urbanization in the North China Plain (NCP), air pollution and extreme haze events frequently occur in this region, the formation of which is closely related to the volatility of aerosol components (Li et al., 2017; Shiraiwa and Seinfeld, 2012). Volatility may also have an impact on the air pollution and haze events in this region. Therefore, it is crucial to understand the volatility of aerosol components in the NCP.

In this study, we compared the effects of the methods of syringe deposition and atomization on T_{max} with a series of authentic organic standards using FIGAERO-LToF-CIMS. Also, we investigated the influences of inorganic salts on T_{max} of organics. In addition, we developed empirical volatility-molecular formula functions based on measured C^* of selected CHO and CHON compounds with various O/C ratios in ambient OA particles, which were collected at Wangdu station in the North China Plain, China, from January 15 to 22, 2019. Our empirical functions were also compared with previous ones.

2 Experimental methods

2.1 FIGAERO-LToF-CIMS

We measured the chemical composition and thermograms of particulate compounds collected on filters via a FIGAERO-LToF-CIMS with a mass resolving power of 7700-8500, and the volatility of compounds was acquired from thermograms (Bertram et al., 2011; Lee et al., 2014; Lopez-Hilfiker et al., 2014). The design and operation of the FIGAERO have been introduced in previous studies (Bannan et al., 2019; Lopez-Hilfiker et al., 2014; Thornton et al., 2020; Ye et al., 2020). In this study, particles collected in the lab calibration experiments or from the field campaign were thermally desorbed utilizing an ultrahigh purity (UHP) nitrogen flow at 2.3 Liter per minute^{-1} (lpm), among which 1.0 lpm UPH N_2 passed the filter and entered the ion-molecule reaction (IMR) chamber. In IMR, organic molecules were charged by iodide ions generated by the exposure of the mixture of CH_3I and UHP N_2 to a 0.1 mCi radioactive Am-241 source. During the thermo-desorption process, the heating temperature ramp started roughly from room temperature (~25 ˚C) to 134 ˚C and then the filter was held at 134 °C for 40 min to ensure that most of the organic compounds had been desorbed from the filter (Lopez-Hilfiker et al., 2016). Most of the ambient organic compounds can be desorbed from the filter at less than 134°C (Huang et al., 2019). During ambient filter measurements, background measurements using a blank filter were also conducted. An example of the background signal of an identified compound was shown in Figure S1.

A Tofware software (version 3.1.2, Tofwerk AG, Switzerland) was used to analyze the data of mass spectrometer. To plot thermograms, signals of evaporated compounds were normalized by the abundance of the reagent ions and then subtracted with the background signals, which were normalized similarly. The raw data was acquired at a frequency of 1 Hz and then averaged to a 20 s time interval during the data analysis. As the desorption features of ambient aerosol particles were quite complex, we applied the Levenberg–Marquardt algorithm to fit the thermograms and conducted peak deconvolution for the multimodal thermograms (Goodman and Brenna, 1994; Lopez-Hilfiker et al., 2015; Stolzenburg et al., 2018). In the case of a multimodal thermogram, the higher-temperature peak(s) (i.e., the warmer peak) was assumed to come from the thermal decomposition of larger molecules or isomers with different vapor pressures (Huang et al., 2018; Wang et al., 2016), hence in this study, T_{max} of the cooler peak (i.e., the first peak) was used to estimate the volatility of an organic compound.

2.2 Calibration experiments

The C^* versus T_{max} calibration curve was obtained by species with known vapor pressures. Two methods referred as the syringe deposition method and the atomization method, were used to prepare filter samples of authentic compounds. For the syringe deposition method, certain amounts of authentic species dissolved in the acetonitrile solvent were injected onto a PTFE filter

https://doi.org/10.5194/acp-2021-1006
Preprint. Discussion started: 5 January 2022

Atmospheric Chemistry and Physics Discussions

by a syringe. While the acetonitrile solvent was supposed to quickly evaporate from the filter and have a minor effect on authentic species, only the authentic species were thermally desorbed during the subsequent FIGAERO-LToF-CIMS analysis. For the atomization method, the authentic species dissolved in deionized water were atomized by a commercial atomizer (TSI® 3076). Atomized particles were diluted and dried by a zero-gas flow and silica gel tubes, after which the relative humidity (RH) of the flow was regulated to around ~ 2% (Figure S2). Then, particles were collected onto a PTFE filter and subsequently analyzed by the FIGAERO-LToF-CIMS. The amount of collected particles can be calculated based on the number size distribution of particles measured by a Scanning Mobility Particle Sizer (SMPS, TSI® 3776), the particle density, the collection time, and the flow rate through the filter (Ylisirniö et al., 2021).

During our laboratory tests, five sets of calibration experiments were conducted. These experiment conditions are summarized in Table 1. One set of (No.1) experiments using the syringe deposition method were performed, where polyethylene glycols (PEGs) were used as authentic organic standards (Bannan et al., 2019). Besides, four sets of atomization experiments were also conducted. The second (No.2) set works as an intercomparison with previous syringe deposition (No.1) experiments. The third, fourth and fifth (No.3-5) set experiments were conducted in order to explore the effect of ammonium sulfate. In these three sets, erythritol, PEG-6, PEG-7, PEG-8, and citric acid were used as authentic organic standards because they can dissolve with ammonium sulfate in deionized water. In the third (No.3) set, ammonium sulfate was not added to the standard solution, and there were only organic standards. In the fourth (No.4) set, ammonium sulfate was mixed with erythritol, PEG-6, PEG-7, PEG-8, and citric acid, respectively. 200 ng atomized particles were collected. It is assumed that the atomized particles were internally mixed with the same mass ratio as that in the solution (Drisdell et al., 2009), consisting of 100 ng of ammonium sulfate and 100 ng of the mixed organic standard. In the fifth (No.5) set, ammonium sulfate was mixed with erythritol, PEG-6, PEG-7, PEG-8, and citric acid together. 1000 ng atomized particles were collected. With the same assumption as mentioned above, the particles consisted of 500 ng of ammonium sulfate and 100 ng of each organic standard. Four replicates were performed for each set of experiments.

Table 1. Conditions of five sets of calibration experiments.

No.	Method	Authentic standards	Concentration	Solvent	Deposited volume	Mass loading
1	Syringe deposition	PEG-4 ($C_8H_{18}O_5$) PEG-5 ($C_{10}H_{22}O_6$) PEG-6 ($C_{12}H_{26}O_7$) PEG-7 ($C_{14}H_{30}O_8$) PEG-8 ($C_{16}H_{34}O_9$)	0.05 g L^{-1} 0.05 g L^{-1} 0.05 g L^{-1} 0.05 g L^{-1} 0.05 g L^{-1}	Acetonitrile	2 µl	100 ng
2	Atomization	PEG-4 ($C_8H_{18}O_5$) PEG-5 ($C_{10}H_{22}O_6$) PEG-6 ($C_{12}H_{26}O_7$) PEG-7 ($C_{14}H_{30}O_8$) PEG-8 ($C_{16}H_{34}O_9$)	1.0 g L^{-1} 1.0 g L^{-1} 1.0 g L^{-1} 1.0 g L^{-1} 1.0 g L^{-1}	Deionized water	/	500 ng
3	Atomization	Erythritol ($C_4H_{10}O_4$) PEG-6 ($C_{12}H_{26}O_7$) PEG-7 ($C_{14}H_{30}O_8$) PEG-8 ($C_{16}H_{34}O_9$) Citric acid ($C_6H_8O_7$)	0.5 g L^{-1} 0.5 g L^{-1} 0.5 g L^{-1} 0.5 g L^{-1} 0.5 g L^{-1}	Deionized water	/	100 ng
4	Atomization	Erythritol ($C_4H_{10}O_4$) +ammonium sulfate PEG-6 ($C_{12}H_{26}O_7$) + ammonium sulfate PEG-7 ($C_{14}H_{30}O_8$) + ammonium sulfate PEG-8 ($C_{16}H_{34}O_9$) + ammonium sulfate Citric acid ($C_6H_8O_7$) + ammonium sulfate	0.5 g L^{-1} + 0.5 g L^{-1} 0.5 g L^{-1} + 0.5 g L^{-1} 0.5 g L^{-1} + 0.5 g L^{-1} 0.5 g L^{-1} + 0.5 g L^{-1} 0.5 g L^{-1} + 0.5 g L^{-1}	Deionized water	/	200 ng (100 ng + 100 ng) 200 ng (100 ng + 100 ng) 200 ng (100 ng + 100 ng) 200 ng (100 ng + 100 ng) 200 ng (100 ng + 100 ng)
5	Atomization	Erythritol ($C_4H_{10}O_4$) + PEG-6 ($C_{12}H_{26}O_7$) +PEG-7 ($C_{14}H_{30}O_8$) + PEG-8 ($C_{16}H_{34}O_9$) + citric acid ($C_6H_8O_7$) + ammonium sulfate	0.5 g L^{-1} + 0.5 g L^{-1} +0.5 g L^{-1} + 0.5 g L^{-1} +0.5 g L^{-1} + 2.5 g L^{-1}	Deionized water	/	1000 ng (100 ng + 100 ng +100 ng +100 ng + 100 ng + 500 ng)

https://doi.org/10.5194/acp-2021-1006
Preprint. Discussion started: 5 January 2022

Atmospheric Chemistry and Physics Discussions

2.3 Field Campaign

An ambient campaign was conducted from December 16, 2018 to January 22, 2019 at Wangdu station, Hebei Province, China (Wang et al., 2020b). The campaign site (38.66°N, 115.19°E) was mainly influenced by the surrounding transportation, industrial and residential sources, and farmlands and forests and can be treated as a typical suburban station.

Aerosol particles ($PM_{2.5}$) were collected four times every day, and each collection lasted for 15 minutes (i.e., 7:00-7:15, 12:00-12:15, 17:30-17:45, and 21:00-21:15 local time, respectively). Ambient $PM_{2.5}$ was sampled onto PTFE filters (5μm pore size, 25 mm diameter, Millipore), and the flow rate was regulated at 1.42 L min^{-1}. After the collection, filter samples were preserved at -20 ˚C in a freezer until further analysis. In this study, 30 filter samples between January 15, 2019 and January 22, 2019 were analyzed. The mass concentration of $PM_{2.5}$ was also measured by a commercial synchronized hybrid real-time particulate monitor (TEI, Model 5030i).

2.4 Saturation mass concentration (C^*)

2.4.1 Calculation of C^*

By correlating the logarithm of P_{sat} at 298K of these authentic standards in the literature to their T_{max} values obtained from the desorption thermograms, a linear relationship can be obtained (Bannan et al., 2019):

$$log_{10}(P_{sat}) = aT_{max} + b, \quad (1)$$

where a and b are fitted parameters, and this expression can also be expressed as:

$$P_{Sat}(pa) = 10^{aT_{max}+b}, \quad (2)$$

On the other hand, P_{sat} can be converted to C^* with the assumption of the ideal gas law (Ylisirniö et al., 2019, 2021). In this way, the relationship between C^* and T_{max} was deduced as:

$$C^*\ (\mu g \cdot m^{-3}) = \frac{(10^{aT_{max}+b})M_w}{RT}10^6, \quad (3)$$

where M_w is the molecular weight of an authentic compound (g mol^{-1}), R is the gas constant (8.314 J mol^{-1} K^{-1}), and T is the temperature when the P_{sat} is determined (K; in our study, T is 298K).

2.4.2 Correlation between C^* and molecular formulas

We substituted the measured T_{max} of selected organic compounds in the ambient aerosol particles into Eq. (3) with fitted a and b values from experiments with authentic standards, and obtained their C^*. Then we correlated C^* to molecular formulas of these selected organic compounds in a function similar to what was developed in a previous study (Donahue et al., 2011; Mohr et al., 2019) :

$$log_{10}\,C_0 = (n_c^0 - n_c)b_c - (n_o - 3n_N)b_o - 2\cdot\frac{(n_o - 3n_N)n_c}{(n_c + n_o - 3n_N)}b_{co} - n_N b_N \quad (4)$$

where n_c^0 is the reference carbon number and set to be 25 (Donahue et al., 2011); n_c, n_o and n_N is numbers of carbon, oxygen and nitrogen atoms in an organic species, respectively; b_c, b_o and b_N denotes the contribution of each kind of atoms to $log_{10}\,C_0$, respectively, and b_{co} is the carbon-oxygen nonideality (Donahue et al., 2011; Li et al., 2016). Values of b_c, b_o, b_N, and b_{co} were fitted with multi-linear least-squares analysis.

3 Results and discussion

3.1 Laboratory Calibration

Figure 1 (and Figure S3) compares the T_{max} values for the same authentic organic standards when using different calibration methods. PEG4 was not detected by CIMS with the second (No.2) set of calibration experiments, which is consistent with the result of a previous study (Ylisirniö et al., 2021). This observation is most likely due to the high volatility of PEG-4 that leads

https://doi.org/10.5194/acp-2021-1006
Preprint. Discussion started: 5 January 2022

Atmospheric Chemistry and Physics Discussions

to its evaporation even before the CIMS measurement (Ylisirniö et al., 2021). The T_{max} values measured with the syringe deposition experiments have larger error bars. The T_{max} may increase with increased filter loadings (Wang and Hildebrandt Ruiz, 2018), if calibrated with the same method. However, despite a larger mass loading (500 ng) in the atomization (No.2) experiments than that (100 ng) in the syringe deposition (No.1) experiments, the T_{max} values measured with the atomization method is about 20 ˚C lower than those with the syringe deposition method for the same compound. This observation can be explained by the fact that the surface area of the material deposited by the syringe is smaller than that of deposited aerosol particles, which requires more time to evaporate and correspond to higher T_{max} values (Ylisirniö et al., 2021).

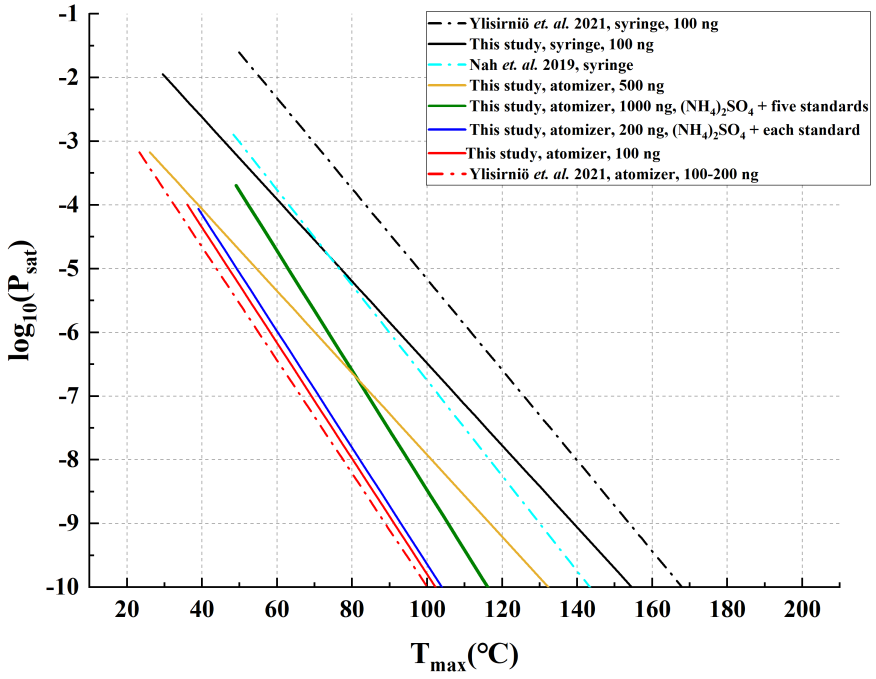

Figure 1. Comparison of calibration results obtained in this study with those reported previously. The solid black line denotes the calibration results obtained with 100 ng deposited PEGs (including PEG-4, PEG-5, PEG-6, PEG-7 and PEG-8) in this study by the syringe method. The solid orange line denotes calibration results obtained with 500 ng deposited PEGs (including PEG-4, PEG-5, PEG-6, PEG-7 and PEG-8) in this study by the atomization method. The solid red line denotes calibration results in the absence of ammonium sulfate obtained with 100 ng deposited erythritol, PEG-6, PEG-7, PEG-8, and citric acid in this study using the atomization method. The solid blue line denotes calibration results obtained by adding ammonium sulfate to erythritol, PEG-6, PEG-7, PEG-8, and citric acid, respectively, in this study using the atomization method, and 200 ng dried particles were collected. The solid green line denotes calibration results for the mixture of ammonium sulfate, erythritol, PEG-6, PEG-7, PEG-8, and citric acid obtained in this study using the atomization method, and 1000 ng dried particles were collected. The light blue dash-dot line denotes calibration results obtained with acids and erythritol by Nah et al., (2019) using the syringe method. The black dash-dot line represents calibration results obtained with 100 ng deposited PEGs (including PEG-4, PEG-5, PEG-6, PEG-7 and PEG-8) by Ylisirniö et al., (2019) using the syringe method. The red dash-dot line denotes calibration results obtained with 100-200 ng deposited PEGs (including PEG-5, PEG-6, PEG-7 and PEG-8) by Ylisirniö et al., (2019) using the atomization method.

The effect of ammonium sulfate on T_{max} of organics is also investigated, as shown in Figure 1 (and Figure S4), since the majority of atmospheric aerosol particles consists of ~50% ammonium sulfate and 50% carbonaceous components (Drisdell

https://doi.org/10.5194/acp-2021-1006
Preprint. Discussion started: 5 January 2022

et al., 2009). Clearly, mixing the same amount of ammonium sulfate with each of the five organic standards, as done in the fourth (No.4) set of calibration experiments, increased the T_{max} values of erythritol and citric acid but did not alter the T_{max} values of PEGs 6-8 significantly. However, mixing ammonium sulfate with five organic compounds together, as done in the fifth (No.5) set of calibration experiments, would increase the T_{max} values of all the five organic standards, among which the T_{max} values of PEGs 6-8 increased by around 20 ˚C. Since there is no obvious difference in T_{max} values between mixed PEGs and stand-alone PEGs, both of which are measured in the absence of ammonium sulfate (Bannan et al., 2019; Ylisirniö et al., 2021), the observed increase in the T_{max} values of five authentic organic standards is likely due to the addition of ammonium sulfate. Ammonium sulfate tends to decrease the volatility of particulate organic compounds, which is likely the cause of the observed matrix effects. A typical example is that the interaction between organic acids and inorganic salts in the particles forms organic salts, which can facilitate the partitioning of organic acids onto the particles (Nie et al., 2017; Yli-Juuti et al., 2013; Zardini et al., 2010). In other words, ammonium sulfate can increase particle viscosity (diffusion limitations within the particles) and interactions of organic and inorganic components within particles (Huang et al., 2018), so that the T_{max} values of authentic organic standards become larger. The extent of this matrix effect may be related to the mass of ammonium sulfate in the particles. The mass of ammonium sulfate was 100 ng in the fourth (No.4) set of calibration experiments whereas this mass was 500 ng in the fifth (No.5) set of experiments. Thus, the T_{max} value, for the same species, measured in the latter case is significantly higher than that measured in the former case. Furthermore, the filter mass loading of the fifth (No.5) set of calibration experiments (1000 ng) was larger than that of the fourth (No.4) set of calibration experiments (200 ng), which may be one of the reasons for the increase in T_{max} value. As there is a synergistic effect between inorganic salts and mass loading, a more detailed study is required.

In Figure 1, we further compare our calibration results with previously reported ones. Five solid calibration lines acquired in this study are located between the dash-dot calibration lines by Ylisirniö et al. (2021) using the atomization method and the syringe deposition method. The solid calibration line obtained with PEGs (O/C > 0.25) by the syringe deposition method in this study is similar to the dash-dot calibration line that was also obtained by the syringe deposition method, but with acids (including acid with O/C < 0.25 and O/C > 0.25) and erythritol (O/C > 0.25) (Nah et al., 2019b), which hints authentic organic standards may have less effect on the calibration line. In addition, the calibration line obtained with 100 ng deposited standards in this study by the atomization method almost overlap that obtained with the same method, standard, and mass loading (Ylisirniö et al., 2021). However, the calibration line obtained with 100 ng deposited standards in this study by the syringe deposition method is far away from the dash-dot calibration line obtained with the same method, standard, and mass loading (Ylisirniö et al., 2021). Clearly, compared with the syringe deposition method, the atomization method shows much better repeatability, even between different studies.

Moreover, the fraction of organic species and inorganic salts of non-refractory submicron aerosol species (NR-PM1) in Beijing in winter 2018 are about 48% and 52%, respectively (Zhou et al., 2020). The fraction of organic species and inorganic salts of total particulate matter (PM) in a rural site (Gucheng in Hebei province) in winter 2018 are about 40% and 60%, respectively (Xu et al., 2021). The mass ratios of the inorganic salt to organic species were close to 1:1 which was similar to that of our laboratory tests (i.e., the fifth (No.5) set of calibration experiments). Furthermore, the median mass loading of 30 filter samples collected in our field campaign were around 1100 ng. We thus used the calibration line obtained by atomizing the mixed solution of ammonium sulfate and five organic standards and collecting 1000 ng particles (the fifth (No.5) set of experiments) to estimate the T_{max} values of organic compounds in ambient particles.

3.2 Volatility of OA components

We identified 1,448 compounds from the filter collected on 7:00-7:15, January 15, 2019, in Wangdu, whose mass defect plot is shown in Figure 2. Among them, 340 CHO and 663 CHON species account for a large proportion of the total signal, owing to iodide-adduct chemical ionization being sensitive toward multifunctional oxygenated organic compounds with minimal fragmentation (Bertram et al., 2011; Lopez-Hilfiker et al., 2016). In addition to 326 other species that have been assigned with molecular formulas but cannot be divided into either the CHO or CHON groups, there are also 119 species without attributed

https://doi.org/10.5194/acp-2021-1006
Preprint. Discussion started: 5 January 2022

Atmospheric Chemistry and Physics Discussions

molecular formulas.

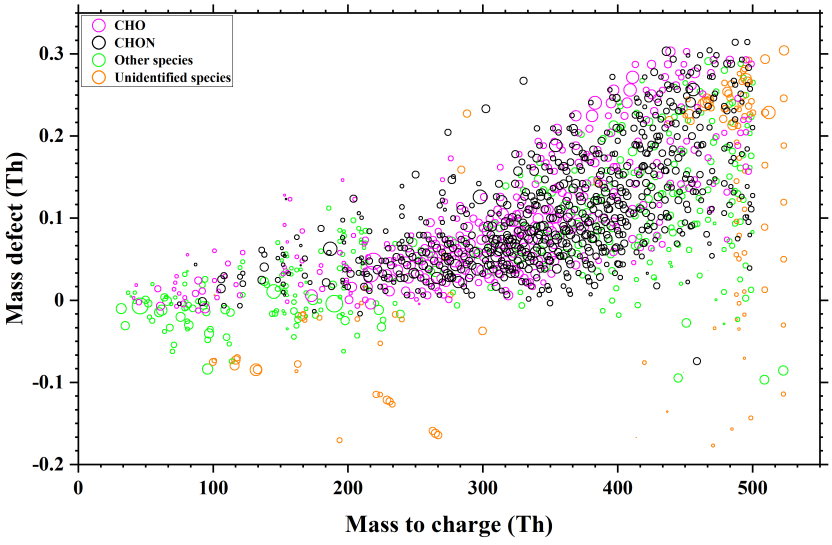

Figure 2. A typical Mass defect plot for compounds desorbed from a filter collected on 7:00-7:15, January 15, 2019, in Wangdu. The symbol size is proportional to the logarithm of signal intensity. The reagent ion (I^-) was not removed from their formulas.

Among the 1,448 species, we can attribute a T_{max} to 765 species whose thermograms are characterized with a distinguishable T_{max} with one or two desorption peaks, as shown in Figure S5a/S5c and Figure S5b/S5d, and the rest whose thermograms did not show a peak and thus the position of T_{max} cannot be judged, as shown in Figure S5e and Figure S5f. In Figure S6, we show the thermal desorption temperature of these 765 particulate compounds during the FIGAERO-LToF-CIMS analysis. The desorption temperatures of these organic compounds mainly concentrated in the 80~100 ˚C range. The thermograms of most organic compounds show a single peak, and the mass-to-charge ratio (m/z) of these compounds are mainly concentrated in the range of 250 ~ 450 Th, and the dominated compounds are $C_{13}H_{25}NO_2$, $C_{16}H_{32}O_2$, $C_{18}H_{35}NO_4$, $C_6H_{10}O_5$, $C_9H_{17}NO_2$ and $C_{18}H_{34}O_2$.

We analyzed 30 filter samples in total. For each filter, we selected species that can be attributed with a reliable molecular formula in the format of either CHO or CHNO, and species that can be designated with a T_{max}, the intersection of which correspond to species with both reliable CHO/CHNO type molecular formulas and T_{max} values. There are 181 such organic compounds including 91 CHO and 90 CHON species that were present in more than 20 out of 30 filter samples. The molecular formula, molecular weight, T_{max}, and C^* calculated according to our calibration in Figure 1 for the 91 CHO and 90 CHON species are summarized in Table S1 and Table S2, respectively.

The evaporation and decomposition of these 181 organic compounds during the FIGAERO analysis are shown in Figure 3. The cooler-temperature in a double-peak thermogram mostly appeared in the green rectangular band of 45~80 ˚C, whereas the higher-temperature one in a double-peak that is mainly the result of thermal decomposition of higher molecular weight organic compounds (Huang et al., 2018), concentrated in the purple rectangular band of 100~125 ˚C, which is consistent with the result of Wang et al. (2016). On the other hand, the corresponding evaporation temperature for a compound with a single-peak thermogram is concentrated in the red rectangular band of 80~100 ˚C. Clearly, the compounds in Figure 3 can be divided into two groups, as illustrated with the two dashed circles. For each group, the T_{max} values of the single peaks and the cooler ones

https://doi.org/10.5194/acp-2021-1006
Preprint. Discussion started: 5 January 2022

Atmospheric Chemistry and Physics Discussions

of a double-peak increase with their corresponding molecular weight, which is consistent with the fact that similar compounds with larger molecular weight tend to possess lower volatility.

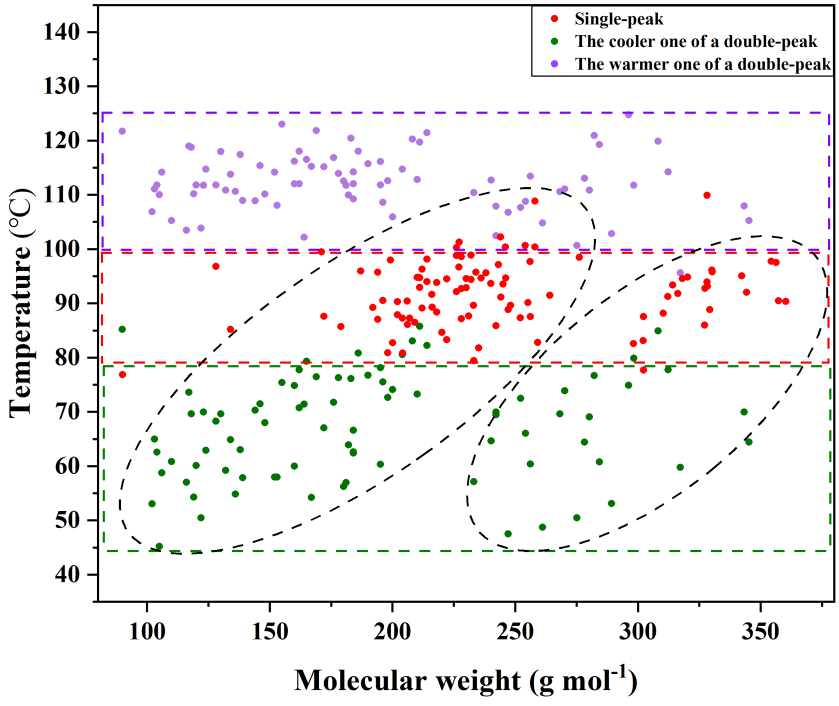

Figure 3. Evaporation and decomposition of 91 CHO and 90 CHON compounds, as illustrated by the temperature of a species' thermogram signal peaks (one or two), of which the reagent ion (I^-) was excluded from their formulas. The signal peaks, the cooler and warmer peaks of double-peaks are denoted by red, green and purple circles, respectively. Rectangular bands depict the temperature zones in which peaks appear.

In Figure 4, the T_{max} values of these 181 compounds are translated into C^* values according to Eq. (3). The data points for the higher-temperature ones in double-peak thermograms that in fact, do not correspond to a T_{max} are removed, and the remaining data points are colour-scaled with their O/C ratios. It is obvious that these organic compounds can still be divided into two groups. The species in the red dashed circle are the same as those in the left dashed circle in Figure 3, whereas the compounds in the blue dashed circle are the same as those in the right dashed circle. The molecular weights of species in the two groups overlapped, although the ones in the red dashed circle are characterized with relative lower molecular weights, and the ones in the blue dashed circle are with relatively higher molecular weights. The O/C ratio can clearly distinguish the two groups: 0.56 ± 0.35 (average ± one standard deviation) for the left group and 0.18 ± 0.08 for the right group, indicating that the O/C ratio of these compounds could be a key parameter.

https://doi.org/10.5194/acp-2021-1006
Preprint. Discussion started: 5 January 2022

Atmospheric Chemistry and Physics Discussions

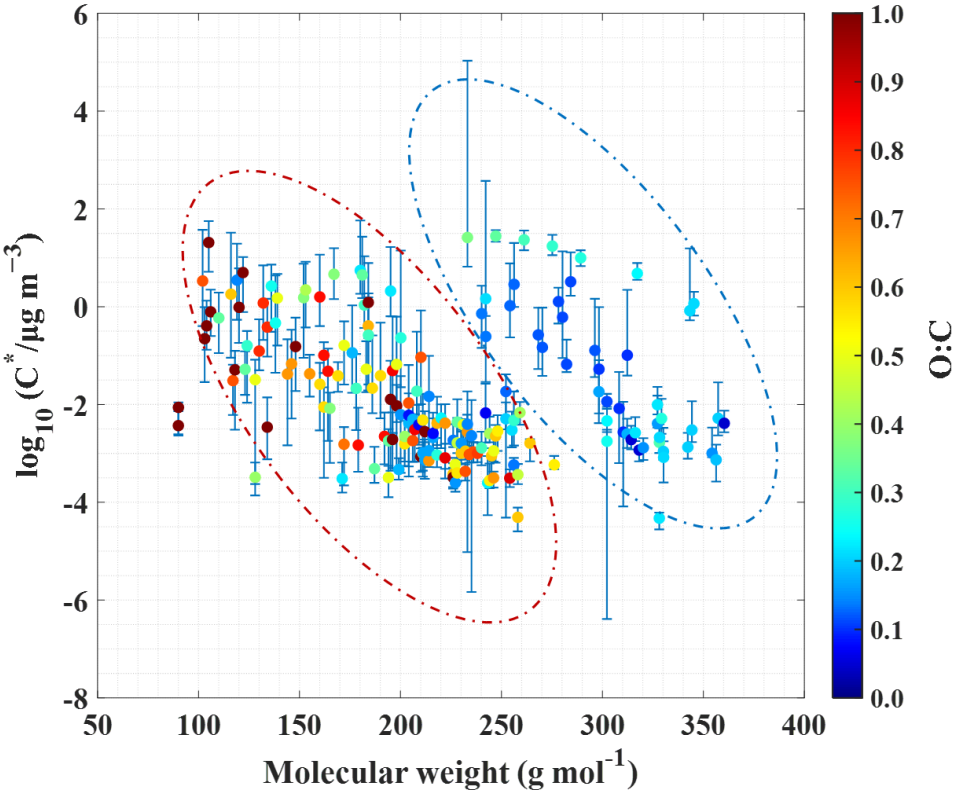

315

Figure 4. Saturation mass concentration of CHO and CHON compounds against their molar masses, as colour-coded by the molecular O/C ratio. Compounds with O/C ratio greater than or equal to 1.0 are marked with the same colour. Whiskers denote 25th and 75th percentile values of measured saturation mass concentration from total of 30 samples. Dashed circles group these compounds with the same key characters.

320

Figure S7 clearly shows the O/C characteristics of compounds in the two regions, where the red triangles correspond to those in the red dashed circle of Figure 4, and the blue circles correspond to those in the blue dashed circle. The O/C ratios of organic compounds in the red dashed circle ranged from 0.25 to 1.0, and the O/C ratios of those in the blue dashed circle varied between 0-0.25. The tentative identification of $C_6H_{10}O_5$ (levoglucosan or related isomers) among compounds in the red dashed circle, 325 which is a well-accepted tracer of biomass burning OA (BBOA) (Gaston et al., 2016), and of $C_{16}H_{32}O_2$ (palmitic acid), $C_{17}H_{34}O_2$ (margaric acid), $C_{18}H_{32}O_2$ (linoleic acid), and $C_{18}H_{34}O_2$ (oleic acid) among the compounds in the blue dashed circle, which have been previously identified as markers of cooking-influenced OA (COA) (Chow et al., 2007; Pei et al., 2016). The correlation coefficient (Pearson's r) between $C_6H_{10}O_5$ and other compounds in the red dashed circle is 0.88 ± 0.18 (average ± one standard deviation), and the correlation coefficient between $C_{18}H_{34}O_2$ and other compounds in the blue dashed circle is 330 0.53 ± 0.14. We show examples of the correlation of $C_6H_{10}O_5$, $C_{18}H_{32}O_2$ and other compounds in Figure S8. Indeed, there are a number of sources of COA and BBOA near the campaign site, and the campaign was carried out during the heating season. Hence, organic compounds in the red dashed circle may be mainly derived from BBOA, and those in the blue dashed circle partly derived from COA.

335 We thus separately optimized the correlation between the molecular elemental composition and the saturation mass concentration of organic compounds in these two regions in Figure 4. As shown in Table 2, the parameterization in Eq. (4-1)

https://doi.org/10.5194/acp-2021-1006
Preprint. Discussion started: 5 January 2022

Atmospheric Chemistry and Physics Discussions

is dedicated for compounds with O/C ratios of 0.25-1, whereas Eq. (4-2) is more suitable for compounds with O/C ratios of 0-0.25. Compared with those from Mohr et al. (2019), our fits are mainly based on semi-volatility organic compounds (SVOCs) and low-volatility organic compounds (LVOCs), which are predominantly in the particle phase in the atmosphere.

Table 2. The improved parameterizations of saturation mass concentration by the least-square optimization from Eq. (4). The best-fit parameters were obtained at 298K. Where the parameter n_c^0 = 25, it is the baseline carbon backbone for the volatility of 1 μg m^{-3} without adding any functional groups (Donahue et al., 2011; Stolzenburg et al., 2018).

	n_c^0	b_c	b_o	b_{co}	b_N	Suggested O/C range
Eq. (4-1)	25	0.0700	0.6307	-0.0615	2.3962	0.25-1
Eq. (4-2)	25	0.2075	2.8276	-1.0744	1.8223	0-0.25

4 Atmospheric implications

For ambient studies, it is crucial to develop a more accurate empirical formula to estimate the volatility of organics in particles. Parametrization in Donahue et al. (2011) is mainly based on mono-functional compounds such as alcohol, aldehyde, acid and etc., and could cause a large uncertainty when estimating volatility of compounds in the range $-5 < \log_{10}(C^*) < 2$ and $1{:}3 < O{:}C < 1{:}1$, because volatilities in this region are extrapolated with volatilities of compounds with simpler molecular formulas (Donahue et al., 2011). In addition, compounds in this region may be characterized with multiple functionalities, which are also lacking as reference standards in the Donahue et al. (2011) study. Compounds in this region can be roughly regarded as oxygenated organic aerosols (OOAs) (Donahue et al., 2011). In our study, a yellow dashed frame is used to mark this region in Figure S7, which is occupied by organic compounds that are concentrated in the red dashed circle of Figure 4. Furthermore, we used the 15 highly oxygenated organic molecules (HOMs) with O/C ratios of 0.25-1 whose volatility was estimated by the SIMPOL method (Pankow and Asher, 2008) in the Tröstl et al., (2016) study as benchmarks to compare the performance of different parameterization methods, as shown in Figure 5(a). As expected, volatilities predicted by the Donahue et al. (2011) parameterization are not consistent with those by the SIMPOL method. Although Mohr et al. (2019) updated parametrization based on those 15 HOMs detected by Tröstl et al., (2016), the volatility predicted by the Mohr et al. (2019) parameterization does not match those by the SIMPOL method very well, which could be explained by not considering covalent binding, using the same parameterization for dimer and monomer may cause deviations. On the other hand, the accuracy of the parameterizations of Stolzenburg et al. (2018), Li et al. (2016), and Eq. (4-1) is generally comparable, although a few data points are more off from the 1:1 line. Stolzenburg et al. (2018) modified parameterization also based on those 15 HOMs and fitted dimer and monomer separately, allowing their parameters to include the covalent binding. Li et al. (2016) developed parameterization based on 31066 compounds from the NCI open database, which contain 8420 CHO compounds with O/C ratios ranging from 0 to 1. Therefore, the parameterizations of Stolzenburg et al. (2018) and Li et al. (2016) agree well with that of the SIMPOL method. The parameterization of Eq. (4-1) based on the compounds in the red dashed circle of Figure 4 contain lots of OOAs species (e.g., 32 HOMs). Thus the Eq. (4-1) can accurately estimate the volatility of ambient OOAs.

https://doi.org/10.5194/acp-2021-1006
Preprint. Discussion started: 5 January 2022

Atmospheric Chemistry and Physics Discussions

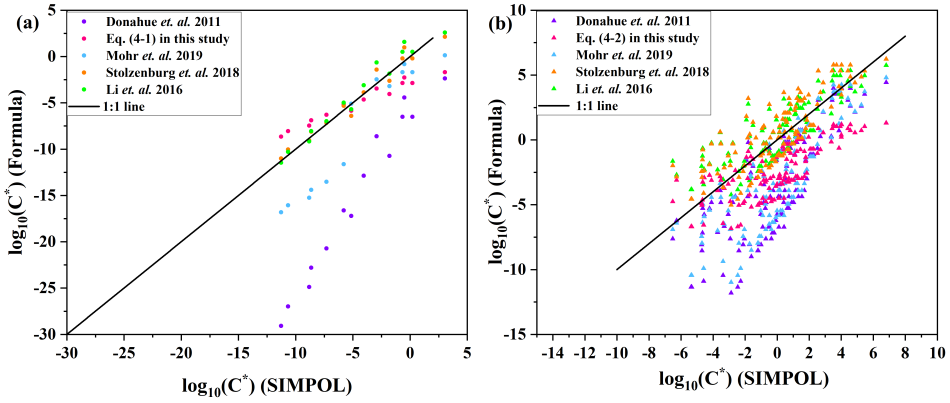

Figure 5. (a) Saturation mass concentration (C^*) of 15 HOMs (O/C:0.25-1) estimated by Eq. (4-1) in this study, and parametrizations from Donahue et al. (2011), Mohr rt al. (2019), Stolzenburg et al. (2018), and Li et al. (2016), respectively, against that estimated by the SIMPOL method. (b) Saturation mass concentration (C^*) of 132 CHO compounds (O/C:0-0.25) estimated by Eq. (4-2) in this study, and parametrizations from Donahue et al. (2011), Mohr et al. (2019), Stolzenburg et al. (2018), and Li et al. (2016), respectively, against that estimated by the SIMPOL method.

We also selected 132 CHO compounds with O/C ratios of 0-0.25 as observed either in this study or from the Zhao et al. (2013) and Mazzoleni et al. (2010) field campaigns, whose saturation mass concentration C^* are estimated by different parameterizations and the SIMPOL method. Common structures and functional groups were selected to calculate the volatility of 132 organic compounds by the SIMPOL method. As shown in Figure 5(b), volatilities predicted by the Donahue et al. (2011) parameterization is quite off those by the SIMPOL method, this is mainly because the parameterization was developed according to higher volatility of organic compounds whose volatilities concentrated in the range of $0 < \log_{10}(C^*) < 9$, but those selected 132 CHO compounds with lower volatility whose volatilities concentrate in the range of $-6 < \log_{10}(C^*) < 6$. Although Mohr et al. (2019) updated parametrization based on those 15 HOMs whose volatilities concentrate in the range of $-11 < \log_{10}(C^*) < 3$, volatilities predicted by Mohr et al. (2019) parameterization still is quite off those by the SIMPOL method. This is mainly because those 132 CHO compounds with lower O/C (0-0.25), but the O/C of those 15 HOMs is 0.25-1. Furthermore, we selected 42 alcohols, aldehydes, acids and diols with O/C ratios of 0-0.25 from NIST, whose saturation mass concentration C^* are estimated by different parameterizations. As shown in Figure S9, the volatilities predicted by the Donahue et al. (2011), Mohr et al. (2019), Stolzenburg et al. (2018) and the Li et al. (2016) parameterizations agree well with values in NIST, showing better agreement than the Eq. (4-2) parameterizations. The reason is that we modified parameterizations based on SVOCs ($10^{-0.5} < C^* \leq 10^{2.5}$) and LVOCs ($10^{-4.5} < C^* \leq 10^{-0.5}$), but these 42 compounds predominantly concentrate in the range of intermediate volatility organic compounds (IVOCs, $10^{2.5} < C^*$) (Schervish and Donahue, 2020). Although the applicability of Li et al. (2016) and Stolzenburg et al. (2018) developed parameterizations is more extensive and can accurately estimate the volatility of single IVOCs, SVOCs, LVOCs and extremely low volatility organic compounds (ELVOCs, $C^* \leq 10^{-4.5}$), the Li et al. (2016) parameterization are statistical results based on the NCI open database, and a large number of organic species are needed. Stolzenburg et al. (2018) parameterization added a free parameter b_{add} that included the covalent binding and yielded different values for monomers and dimers. Compared with previous volatility parameterizations, the improved Eq. (4-1) and Eq. (4-2) in this study can better estimate the volatility of SVOCs and LVOCs in the ambient organic aerosols. The volatility estimated by the Eq. (4-2) parameterization is lower than that estimated by the Li et al. (2016) and Stolzenburg et al. (2018) parameterizations, this may be because the matrix effect of inorganic salts has a more obvious effect on organic compounds with large molecular weights, which is supported by the result of calibration experiments that the increase in the T_{max} of PEG-6 (molecular weight: 282.33 Da), PEG-7 (molecular weight: 326.39 Da) and PEG-8 (molecular weight: 370.44 Da) is greater than that of erythritol (molecular weight: 122.12 Da) and citric acid (molecular weight: 192.12 Da) in the fifth (No.5) set of calibration experiments, as shown in Figure S4. And the Eq. (4-2) parameterization

https://doi.org/10.5194/acp-2021-1006
Preprint. Discussion started: 5 January 2022

405 are developed based on organic compounds with large molecular weights in the blue dashed circle of Figure 4. Therefore, it is reasonable that there is a certain discrepancy between the volatility estimated by the improved Eq. (4-1) and Eq. (4-2) based on organic compounds in ambient particles and estimated by the modified parameterizations of Li et al. (2016) and Stolzenburg et al. (2018) based on single and several mixed organic compounds.

410 In summary, our study developed empirical volatility-molecular formula functions (Eq. (4-1) and the Eq. (4-2)), based on measured C^* of selected CHO and CHON compounds in ambient particles. The Eq. (4-1) can more accurately predict the volatility of SVOCs and LVOCs with higher O/C (0.25-1). The Eq. (4-2) can more accurately predict the volatility of SVOCs and LVOCs with lower O/C (0-0.25) in the ambient organic aerosols. The comparison with previous empirical functions suggests that it is feasible to modify empirical functions based on atmospheric organic compounds with unknown structures
415 and functional groups. When analyzing the volatility of atmospheric organic aerosols, it is more reasonable and scientific to add inorganic salts to organic standards and use the atomization method to create the calibration curve because inorganic salts account for around half of atmospheric organic aerosols particles and the effect of inorganic salts is not negligible. Compared with the syringe deposition method, the atomization method shows much better repeatability. Furthermore, we suggest there should be specialized volatility parameterization for different O/C compounds.

420

Data availability. More detailed data can be provided by contacting the corresponding authors.

425

Author contributions. LW designed the study. GY, YLL and YQL conducted the field campaign. SR, YW, YYL, LHW, GY and YLL carried out laboratory experiments. SR analyzed the data. SR, LW and LY wrote the paper with contributions from all of the other co-authors.

430 *Competing interest.* The authors declare that they have no conflicts of interest.

Acknowledgement. This research has been supported by the National Natural Science Foundation of China (21925601 and 92044301).

https://doi.org/10.5194/acp-2021-1006
Preprint. Discussion started: 5 January 2022

References

Bannan, T. J., Le Breton, M., Priestley, M., Worrall, S. D., Bacak, A., Marsden, N. A., Mehra, A., Hammes, J., Hallquist, M., Alfarra, M. R., Krieger, U. K., Reid, J. P., Jayne, J., Robinson, W., McFiggans, G., Coe, H., Percival, C. J. and Topping, D.: A method for extracting calibrated volatility information from the FIGAERO-HR-ToF-CIMS and its experimental application, Atmos. Meas. Tech., 12(3), 1429–1439, doi:10.5194/amt-12-1429-2019, 2019.

Bertram, T. H., Kimmel, J. R., Crisp, T. A., Ryder, O. S., Yatavelli, R. L. N., Thornton, J. A., Cubison, M. J., Gonin, M. and Worsnop, D. R.: A field-deployable, chemical ionization time-of-flight mass spectrometer, Atmos. Meas. Tech., doi:10.5194/amt-4-1471-2011, 2011.

Capouet, M. and Müller, J. F.: A group contribution method for estimating the vapour pressures of α-pinene oxidation products, Atmos. Chem. Phys., doi:10.5194/acp-6-1455-2006, 2006.

Chow, J. C., Watson, J. G., Lowenthal, D. H., Chen, L. W. A., Zielinska, B., Mazzoleni, L. R. and Magliano, K. L.: Evaluation of organic markers for chemical mass balance source apportionment at the Fresno Supersite, Atmos. Chem. Phys., doi:10.5194/acp-7-1741-2007, 2007.

Donahue, N. M., Robinson, A. L., Stanier, C. O. and Pandis, S. N.: Coupled partitioning, dilution, and chemical aging of semivolatile organics, Environ. Sci. Technol., 40(8), 2635–2643, doi:10.1021/es052297c, 2006.

Donahue, N. M., Epstein, S. A., Pandis, S. N. and Robinson, A. L.: A two-dimensional volatility basis set: 1. organic-aerosol mixing thermodynamics, Atmos. Chem. Phys., 11(7), 3303–3318, doi:10.5194/acp-11-3303-2011, 2011.

Drisdell, W. S., Saykally, R. J. and Cohen, R. C.: On the evaporation of ammonium sulfate solution, Proc. Natl. Acad. Sci. U. S. A., 106(45), 18897–18901, doi:10.1073/pnas.0907988106, 2009.

Eichler, P., Müller, M., D'Anna, B. and Wisthaler, A.: A novel inlet system for online chemical analysis of semi-volatile submicron particulate matter, Atmos. Meas. Tech., 8(3), 1353–1360, doi:10.5194/amt-8-1353-2015, 2015.

Faulhaber, A. E., Thomas, B. M., Jimenez, J. L., Jayne, J. T., Worsnop, D. R. and Ziemann, P. J.: Characterization of a thermodenuder-particle beam mass spectrometer system for the study of organic aerosol volatility and composition, Atmos. Meas. Tech., 2(1), 15–31, doi:10.5194/amt-2-15-2009, 2009.

Gaston, C. J., Lopez-Hilfiker, F. D., Whybrew, L. E., Hadley, O., McNair, F., Gao, H., Jaffe, D. A. and Thornton, J. A.: Online molecular characterization of fine particulate matter in Port Angeles, WA: Evidence for a major impact from residential wood smoke, Atmos. Environ., 138, 99–107, doi:10.1016/j.atmosenv.2016.05.013, 2016.

Goodman, K. J. and Brenna, J. T.: Curve Fitting for Restoration of Accuracy for Overlapping Peaks in Gas Chromatography/Combustion Isotope Ratio Mass Spectrometry, Anal. Chem., doi:10.1021/ac00080a015, 1994.

Huang, W., Saathoff, H., Pajunoja, A., Shen, X., Naumann, K. H., Wagner, R., Virtanen, A., Leisner, T. and Mohr, C.: α-Pinene secondary organic aerosol at low temperature: Chemical composition and implications for particle viscosity, Atmos. Chem. Phys., 18(4), 2883–2898, doi:10.5194/acp-18-2883-2018, 2018.

Huang, W., Saathoff, H., Shen, X., Ramisetty, R., Leisner, T. and Mohr, C.: Seasonal characteristics of organic aerosol chemical composition and volatility in Stuttgart, Germany, Atmos. Chem. Phys., 19(18), 11687–11700, doi:10.5194/acp-19-11687-2019, 2019.

Lee, B. H., Lopez-Hilfiker, F. D., Mohr, C., Kurtén, T., Worsnop, D. R. and Thornton, J. A.: An iodide-adduct high-resolution time-of-flight chemical-ionization mass spectrometer: Application to atmospheric inorganic and organic compounds, Environ. Sci. Technol., 48(11), 6309–6317, doi:10.1021/es500362a, 2014.

Li, H., Zhang, Q., Zhang, Q., Chen, C., Wang, L., Wei, Z., Zhou, S., Parworth, C., Zheng, B., Canonaco, F., Prévôt, A. S. H., Chen, P., Zhang, H., Wallington, T. J. and He, K.: Wintertime aerosol chemistry and haze evolution in an extremely polluted city of the North China Plain: Significant contribution from coal and biomass combustion, Atmos. Chem. Phys., 17(7), 4751–4768, doi:10.5194/acp-17-4751-2017, 2017.

Li, Y., Pöschl, U. and Shiraiwa, M.: Molecular corridors and parameterizations of volatility in the chemical evolution of organic aerosols, Atmos. Chem. Phys., 16(5), 3327–3344, doi:10.5194/acp-16-3327-2016, 2016.

Lopez-Hilfiker, F. D., Mohr, C., Ehn, M., Rubach, F., Kleist, E., Wildt, J., Mentel, T. F., Lutz, A., Hallquist, M., Worsnop, D. and Thornton, J. A.: A novel method for online analysis of gas and particle composition: Description and evaluation of a filter inlet for gases and AEROsols (FIGAERO), Atmos. Meas. Tech., 7(4), 983–1001, doi:10.5194/amt-7-983-2014, 2014.

https://doi.org/10.5194/acp-2021-1006
Preprint. Discussion started: 5 January 2022

Lopez-Hilfiker, F. D., Mohr, C., Ehn, M., Rubach, F., Kleist, E., Wildt, J., Mentel, T. F., Carrasquillo, A. J., Daumit, K. E., Hunter, J. F., Kroll, J. H., Worsnop, D. R. and Thornton, J. A.: Phase partitioning and volatility of secondary organic aerosol components formed from α-pinene ozonolysis and OH oxidation: The importance of accretion products and other low volatility compounds, Atmos. Chem. Phys., 15(14), 7765–7776, doi:10.5194/acp-15-7765-2015, 2015.

Lopez-Hilfiker, F. D., Mohr, C., D'Ambro, E. L., Lutz, A., Riedel, T. P., Gaston, C. J., Iyer, S., Zhang, Z., Gold, A., Surratt, J. D., Lee, B. H., Kurten, T., Hu, W. W., Jimenez, J., Hallquist, M. and Thornton, J. A.: Molecular Composition and Volatility of Organic Aerosol in the Southeastern U.S.: Implications for IEPOX Derived SOA, Environ. Sci. Technol., 50(5), 2200–2209, doi:10.1021/acs.est.5b04769, 2016.

Mazzoleni, L. R., Ehrmann, B. M., Shen, X., Marshall, A. G. and Collett, J. L.: Water-soluble atmospheric organic matter in fog: Exact masses and chemical formula identification by ultrahigh-resolution fourier transform ion cyclotron resonance mass spectrometry, Environ. Sci. Technol., doi:10.1021/es903409k, 2010.

Mohr, C., Thornton, J. A., Heitto, A., Lopez-Hilfiker, F. D., Lutz, A., Riipinen, I., Hong, J., Donahue, N. M., Hallquist, M., Petäjä, T., Kulmala, M. and Yli-Juuti, T.: Molecular identification of organic vapors driving atmospheric nanoparticle growth, Nat. Commun., 10(1), 1–7, doi:10.1038/s41467-019-12473-2, 2019.

Nah, T., Xu, L., Osborne-Benthaus, K. A., White, S. M., France, S. and Lee Ng, N.: Mixing order of sulfate aerosols and isoprene epoxydiols affects secondary organic aerosol formation in chamber experiments, Atmos. Environ., 217(September), doi:10.1016/j.atmosenv.2019.116953, 2019a.

Nah, T., Xu, L., Osborne-Benthaus, K. A., White, S. M., France, S. and Lee Ng, N.: Mixing order of sulfate aerosols and isoprene epoxydiols affects secondary organic aerosol formation in chamber experiments, Atmos. Environ., doi:10.1016/j.atmosenv.2019.116953, 2019b.

Nie, W., Hong, J., Häme, S. A. K., Ding, A., Li, Y., Yan, C., Hao, L., Mikkilä, J., Zheng, L., Xie, Y., Zhu, C., Xu, Z., Chi, X., Huang, X., Zhou, Y., Lin, P., Virtanen, A., Worsnop, D. R., Kulmala, M., Ehn, M., Yu, J., Kerminen, V. M. and Petäjä, T.: Volatility of mixed atmospheric humic-like substances and ammonium sulfate particles, Atmos. Chem. Phys., 17(5), 3659–3672, doi:10.5194/acp-17-3659-2017, 2017.

Nizkorodov, S. A., Laskin, J. and Laskin, A.: Molecular chemistry of organic aerosols through the application of high resolution mass spectrometry, Phys. Chem. Chem. Phys., doi:10.1039/c0cp02032j, 2011.

Pankow, J. F.: An absorption model of gas/particle partitioning of organic compounds in the atmosphere, Atmos. Environ., doi:10.1016/1352-2310(94)90093-0, 1994.

Pankow, J. F. and Asher, W. E.: SIMPOL.1: A simple group contribution method for predicting vapor pressures and enthalpies of vaporization of multifunctional organic compounds, Atmos. Chem. Phys., 8(10), 2773–2796, doi:10.5194/acp-8-2773-2008, 2008.

Pei, B., Cui, H., Liu, H. and Yan, N.: Chemical characteristics of fine particulate matter emitted from commercial cooking, Front. Environ. Sci. Eng., doi:10.1007/s11783-016-0829-y, 2016.

Schervish, M. and Donahue, N. M.: Peroxy radical chemistry and the volatility basis set, Atmos. Chem. Phys., doi:10.5194/acp-20-1183-2020, 2020.

Shiraiwa, M. and Seinfeld, J. H.: Equilibration timescale of atmospheric secondary organic aerosol partitioning, Geophys. Res. Lett., doi:10.1029/2012GL054008, 2012.

Smith, J. N., Moore, K. F., McMurry, P. H. and Eisele, F. L.: Atmospheric Measurements of Sub-20 nm Diameter Particle Chemical Composition by Thermal Desorption Chemical Ionization Mass Spectrometry, Aerosol Sci. Technol., 38(2), 100–110, doi:10.1080/02786820490249036, 2004.

Stark, H., Yatavelli, R. L. N., Thompson, S. L., Kang, H., Krechmer, J. E., Kimmel, J. R., Palm, B. B., Hu, W., Hayes, P. L., Day, D. A., Campuzano-Jost, P., Canagaratna, M. R., Jayne, J. T., Worsnop, D. R. and Jimenez, J. L.: Impact of Thermal Decomposition on Thermal Desorption Instruments: Advantage of Thermogram Analysis for Quantifying Volatility Distributions of Organic Species, Environ. Sci. Technol., 51(15), 8491–8500, doi:10.1021/acs.est.7b00160, 2017.

Stocker, T. F., D. Qin, G.-K., Plattner, M. T., Allen, S. K., Boschung, J., Nauels, A., Xia, Y., Bex, V. and Midgley, P. M.: IPCC, 2013: Summary for Policymakers. In: Climate Change 2013: The Physical Science Basis. Contribution of Working Group I to the Fifth Assessment Report of the IPCC., 2013.

https://doi.org/10.5194/acp-2021-1006
Preprint. Discussion started: 5 January 2022

Stolzenburg, D., Fischer, L., Vogel, A. L., Heinritzi, M., Schervish, M., Simon, M., Wagner, A. C., Dada, L., Ahonen, L. R., Amorim, A., Baccarini, A., Bauer, P. S., Baumgartner, B., Bergen, A., Bianchi, F., Breitenlechner, M., Brilke, S., Mazon, S. B., Chen, D., Dias, A., Draper, D. C., Duplissy, J., Haddad, I. El, Finkenzeller, H., Frege, C., Fuchs, C., Garmash, O., Gordon, H., He, X., Helm, J., Hofbauer, V., Hoyle, C. R., Kim, C., Kirkby, J., Kontkanen, J., Kürten, A., Lampilahti, J., Lawler, M., Lehtipalo, K., Leiminger, M., Mai, H., Mathot, S., Mentler, B., Molteni, U., Nie, W., Nieminen, T., Nowak, J. B., Ojdanic, A., Onnela, A., Passananti, M., Petäjä, T., Quéléver, L. L. J., Rissanen, M. P., Sarnela, N., Schallhart, S., Tauber, C., Tomé, A., Wagner, R., Wang, M., Weitz, L., Wimmer, D., Xiao, M., Yan, C., Ye, P., Zha, Q., Baltensperger, U., Curtius, J., Dommen, J., Flagan, R. C., Kulmala, M., Smith, J. N., Worsnop, D. R., Hansel, A., Donahue, N. M. and Winkler, P. M.: Rapid growth of organic aerosol nanoparticles over a wide tropospheric temperature range, Proc. Natl. Acad. Sci. U. S. A., 115(37), 9122–9127, doi:10.1073/pnas.1807604115, 2018.

Thornton, J. A., Mohr, C., Schobesberger, S., D'Ambro, E. L., Lee, B. H. and Lopez-Hilfiker, F. D.: Evaluating Organic Aerosol Sources and Evolution with a Combined Molecular Composition and Volatility Framework Using the Filter Inlet for Gases and Aerosols (FIGAERO), Acc. Chem. Res., doi:10.1021/acs.accounts.0c00259, 2020.

Tröstl, J., Chuang, W. K., Gordon, H., Heinritzi, M., Yan, C., Molteni, U., Ahlm, L., Frege, C., Bianchi, F., Wagner, R., Simon, M., Lehtipalo, K., Williamson, C., Craven, J. S., Duplissy, J., Adamov, A., Almeida, J., Bernhammer, A. K., Breitenlechner, M., Brilke, S., Dias, A., Ehrhart, S., Flagan, R. C., Franchin, A., Fuchs, C., Guida, R., Gysel, M., Hansel, A., Hoyle, C. R., Jokinen, T., Junninen, H., Kangasluoma, J., Keskinen, H., Kim, J., Krapf, M., Kürten, A., Laaksonen, A., Lawler, M., Leiminger, M., Mathot, S., Möhler, O., Nieminen, T., Onnela, A., Petäjä, T., Piel, F. M., Miettinen, P., Rissanen, M. P., Rondo, L., Sarnela, N., Schobesberger, S., Sengupta, K., Sipilä, M., Smith, J. N., Steiner, G., Tomè, A., Virtanen, A., Wagner, A. C., Weingartner, E., Wimmer, D., Winkler, P. M., Ye, P., Carslaw, K. S., Curtius, J., Dommen, J., Kirkby, J., Kulmala, M., Riipinen, I., Worsnop, D. R., Donahue, N. M. and Baltensperger, U.: The role of low-volatility organic compounds in initial particle growth in the atmosphere, Nature, 533(7604), 527–531, doi:10.1038/nature18271, 2016.

Wang, D. S. and Hildebrandt Ruiz, L.: Chlorine-initiated oxidation of alkanes under high-NO conditions: Insights into secondary organic aerosol composition and volatility using a FIGAERO-CIMS, Atmos. Chem. Phys., 18(21), 15535–15553, doi:10.5194/acp-18-15535-2018, 2018.

Wang, M., Yao, L., Zheng, J., Wang, X., Chen, J., Yang, X., Worsnop, D. R., Donahue, N. M. and Wang, L.: Reactions of Atmospheric Particulate Stabilized Criegee Intermediates Lead to High-Molecular-Weight Aerosol Components, Environ. Sci. Technol., 50(11), 5702–5710, doi:10.1021/acs.est.6b02114, 2016.

Wang, M., Chen, D., Xiao, M., Ye, Q., Stolzenburg, D., Hofbauer, V., Ye, P., Vogel, A. L., Mauldin, R. L., Amorim, A., Baccarini, A., Baumgartner, B., Brilke, S., Dada, L., Dias, A., Duplissy, J., Finkenzeller, H., Garmash, O., He, X. C., Hoyle, C. R., Kim, C., Kvashnin, A., Lehtipalo, K., Fischer, L., Molteni, U., Petäjä, T., Pospisilova, V., Quéléver, L. L. J., Rissanen, M., Simon, M., Tauber, C., Tomé, A., Wagner, A. C., Weitz, L., Volkamer, R., Winkler, P. M., Kirkby, J., Worsnop, D. R., Kulmala, M., Baltensperger, U., Dommen, J., El-Haddad, I. and Donahue, N. M.: Photo-oxidation of Aromatic Hydrocarbons Produces Low-Volatility Organic Compounds, Environ. Sci. Technol., 54(13), 7911–7921, doi:10.1021/acs.est.0c02100, 2020a.

Wang, Y., Mehra, A., Krechmer, J. E., Yang, G., Hu, X., Lu, Y., Lambe, A., Canagaratna, M., Chen, J., Worsnop, D., Coe, H. and Wang, L.: Oxygenated products formed from OH-initiated reactions of trimethylbenzene: Autoxidation and accretion, Atmos. Chem. Phys., doi:10.5194/acp-20-9563-2020, 2020b.

Xu, W., Chen, C., Qiu, Y., Li, Y., Zhang, Z., Karnezi, E., Pandis, S. N., Xie, C., Li, Z., Sun, J., Ma, N., Xu, W., Fu, P., Wang, Z., Zhu, J., Worsnop, D. R., Lee Ng, N. and Sun, Y.: Organic aerosol volatility and viscosity in the North China Plain: Contrast between summer and winter, Atmos. Chem. Phys., 21(7), 5463–5476, doi:10.5194/acp-21-5463-2021, 2021.

Yatavelli, R. L. N. and Thornton, J. A.: Particulate organic matter detection using a micro-orifice volatilization impactor coupled to a chemical ionization mass spectrometer (MOVI-CIMS), Aerosol Sci. Technol., doi:10.1080/02786820903380233, 2010.

Ye, C., Yuan, B., Lin, Y., Wang, Z., Hu, W., Li, T., Chen, W., Wu, C., Wang, C., Huang, S., Qi, J., Wang, B., Wang, C., Song, W., Wang, X., Zheng, E., Krechmer, J., Ye, P., Zhang, Z., Wang, X., Worsnop, D. and Shao, M.: Chemical characterization of oxygenated organic compounds in gas-phase and particle-phase using iodide-CIMS with FIGAERO in

https://doi.org/10.5194/acp-2021-1006
Preprint. Discussion started: 5 January 2022

urban air, Atmos. Chem. Phys., (November), 1–62, doi:10.5194/acp-2020-1187, 2020.

Ye, Q., Wang, M., Hofbauer, V., Stolzenburg, D., Chen, D., Schervish, M., Vogel, A., Mauldin, R. L., Baalbaki, R., Brilke, S., Dada, L., Dias, A., Duplissy, J., El Haddad, I., Finkenzeller, H., Fischer, L., He, X., Kim, C., Kürten, A., Lamkaddam, H., Lee, C. P., Lehtipalo, K., Leiminger, M., Manninen, H. E., Marten, R., Mentler, B., Partoll, E., Petäjä, T., Rissanen, M., Schobesberger, S., Schuchmann, S., Simon, M., Tham, Y. J., Vazquez-Pufleau, M., Wagner, A. C., Wang, Y., Wu, Y., Xiao, M., Baltensperger, U., Curtius, J., Flagan, R., Kirkby, J., Kulmala, M., Volkamer, R., Winkler, P. M., Worsnop, D. and Donahue, N. M.: Molecular Composition and Volatility of Nucleated Particles from α-Pinene Oxidation between -50 °c and +25 °c, Environ. Sci. Technol., 53(21), 12357–12365, doi:10.1021/acs.est.9b03265, 2019.

Yli-Juuti, T., Zardini, A. A., Eriksson, A. C., Hansen, A. M. K., Pagels, J. H., Swietlicki, E., Svenningsson, B., Glasius, M., Worsnop, D. R., Riipinen, I. and Bilde, M.: Volatility of organic aerosol: Evaporation of ammonium sulfate/succinic acid aqueous solution droplets, Environ. Sci. Technol., doi:10.1021/es401233c, 2013.

Ylisirniö, A., Buchholz, A., Mohr, C., Li, Z., Barreira, L., Lambe, A., Faiola, C., Kari, E., Yli-Juuti, T., Nizkorodov, S., Worsnop, D., Virtanen, A. and Schobesberger, S.: Composition and volatility of SOA formed from oxidation of real tree emissions compared to single VOC-systems, Atmos. Chem. Phys. Discuss., (October), 1–29, doi:10.5194/acp-2019-939, 2019.

Ylisirniö, A., Barreira, L. M. F., Pullinen, I., Buchholz, A., Jayne, J., Krechmer, J. E., Worsnop, D. R., Virtanen, A. and Schobesberger, S.: On the calibration of FIGAERO-ToF-CIMS: Importance and impact of calibrant delivery for the particle-phase calibration, Atmos. Meas. Tech., 14(1), 355–367, doi:10.5194/amt-14-355-2021, 2021.

Zardini, A. A., Riipinen, I., Koponen, I. K., Kulmala, M. and Bilde, M.: Evaporation of ternary inorganic/organic aqueous droplets: Sodium chloride, succinic acid and water, J. Aerosol Sci., doi:10.1016/j.jaerosci.2010.05.003, 2010.

Zhao, Y., Hallar, A. G. and Mazzoleni, L. R.: Atmospheric organic matter in clouds: Exact masses and molecular formula identification using ultrahigh-resolution FT-ICR mass spectrometry, Atmos. Chem. Phys., 13(24), 12343–12362, doi:10.5194/acp-13-12343-2013, 2013.

Zhou, W., Xu, W., Kim, H., Zhang, Q., Fu, P., Worsnop, D. R. and Sun, Y.: A review of aerosol chemistry in Asia: Insights from aerosol mass spectrometer measurements, Environ. Sci. Process. Impacts, 22(8), 1616–1653, doi:10.1039/d0em00212g, 2020.